Testing Gravity at Short Distances

S. J. Smullin, A. A. Geraci, D. M. Weld, A. Kapitulnik
Department of Physics, Stanford University, Stanford, CA 94025, USA
J. Chiaverini
National Institute of Standards and Technology, Boulder, CO 80305, USA

Various theories of physics beyond the Standard Model, including attempts to resolve the hierarchy problem, include deviations from Newtonian gravity at short distances. Tabletop measurements of gravity can provide constraints on these theories. We have built an apparatus to measure the force between masses separated by tens of microns. The experiment utilizes a micromachined silicon cantilever as a force sensor and small pieces of gold as masses. In this paper, the experimental apparatus and procedure are described.

1. INTRODUCTION

Most people think they know something about gravity and the science surrounding it. Perhaps they know that it is because of gravity that things fall to the ground and maybe they have even heard the story of Isaac Newton being inspired by a falling apple. From billboards, tshirts, and coffee mugs, people know of Albert Einstein and his theory of relativity. In spite of this great popular recognition, gravity is still poorly understood by physicists. Gravity, alone among the four forces in nature, does not fit into the Standard Model that otherwise encompasses observed particles and forces. The challenge to describe gravity with the same tools used to describe Standard Model forces has led to dozens of theories, none of which has been proven and many of which cannot be experimentally tested.

Relativistic corrections aside, what Newton told us about 300 years ago still holds true:

$$V = -\frac{Gm_1m_2}{r}, \tag{1}$$

where G is the gravitational constant and V is the gravitational potential between point masses m_1 and m_2 separated by distance r. Though the predictive power and accuracy of this description has been proven, the unresolved hierarchy problem — the relative weakness of gravity in comparison to the other forces in nature — and the lack of a quantum description of gravity suggest that something may be missing in the Newtonian description of non-relativistic gravity. With these questions in mind, the goal of this experiment is to measure the force between masses separated by submillimeter distances in order to put constraints on deviations from Newtonian gravity. Results are parameterized in terms of a Yukawa potential in addition to the Newtonian gravitational potential:

$$V = -\frac{Gm_1m_2}{r}(1 + \alpha e^{-r/\lambda}). \tag{2}$$

Here, α is the relative strength of the Yukawa potential in comparison to the Newtonian potential and λ is the length scale at which the Yukawa potential becomes relevant.

A Yukawa potential with α and λ in a range that may be experimentally accessible arises in predictions of exotic particles[1–3] (where λ is the Compton wavelength of the particle) and in theories of extra dimensions (where λ is related to the radius of compactification of the extra dimensions)[4]. Reasonable predictions for α and λ cover much of the parameter space untested by experiment. Only recently have measurements of the gravitational force[5–7] or the Casimir force[8] begun to constrain theories in the submillimeter range with $\alpha < 10^{12}$. While many predictions of new physics will have to wait for collider tests to be verified or discarded, tabletop tests of gravity can provide useful experimental constraints now. Though the particular theory of large extra dimensions[4] that originally motivated this work has been constrained past the point of current experimental accessibility by astronomical analysis[9], a measurement of gravity at short distances is a very general test of physics beyond the Standard Model. Ref. [10] provides an excellent review of the theoretical motivations for and experimental progress in tests of the inverse-square force law. Recent experimental results and some theoretical predictions are diagrammed in Fig. 1.

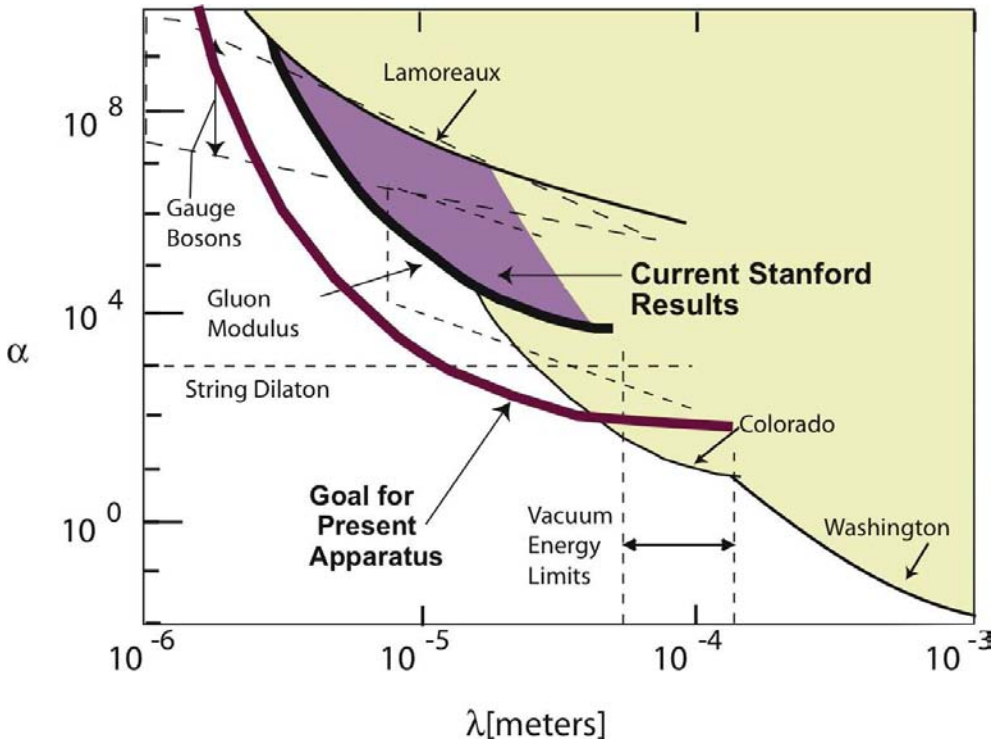

Figure 1: Parameter space showing experimental results (in solid lines) from Refs. [5–8] and some theoretical predictions (dashed lines) from Refs. [1, 3, 4, 11]. The shaded areas show where experimental results have ruled out the possibility of Yukawa-type deviations from Newtonian gravity. Note that different versions of some of these predictions are shown in Ref. [12]. The Stanford data shown are those published in Ref. [7] and the goal is the expected thermal noise limit of the apparatus described in this paper.

2. EXPERIMENTAL DESIGN

In order to measure small forces at short distances, masses are sized comparably to the distance between the masses and a micromachined silicon cantilever is employed as a force sensor. On the end of the cantilever sits a small gold test mass. As shown schematically in Fig. 2, an alternating pattern of gold and silicon bars is oscillated underneath the cantilever, tens of microns away from the test mass. Due to the difference in mass density between gold and silicon, this oscillation creates an alternating gravitational field at the test mass. The coupling between this field and the test mass will cause the test mass to move up and down, driving the cantilever. A measurement of the test mass motion is then used to deduce the force between the masses. A standard fiber interferometer measures the motion of the test mass. A gold-coated silicon-nitride shield between the test mass and the drive mass helps to isolate the test mass from non-gravitational couplings between the gold masses. The entire probe is enclosed in a vacuum can inside of a ^{4}He cryostat. The first version of this experiment is described in detail in Ref. [13], with the first results published in Ref. [7].

2.1. Cantilever

A cantilever behaves like a spring, obeying Hooke's law $F = -kx$, where F is a dc force driving the cantilever, k is the spring constant, and x is the displacement of the cantilever. The dc Newtonian gravitational force in this experiment is of order 10^{-19} N, and the spring constant of the cantilever is close to 0.005 N/m; the gravitational force between these masses would create a very small change in the static position of the cantilever, easily swamped by other dc forces such as the coupling between the test mass and the earth's gravitational field.

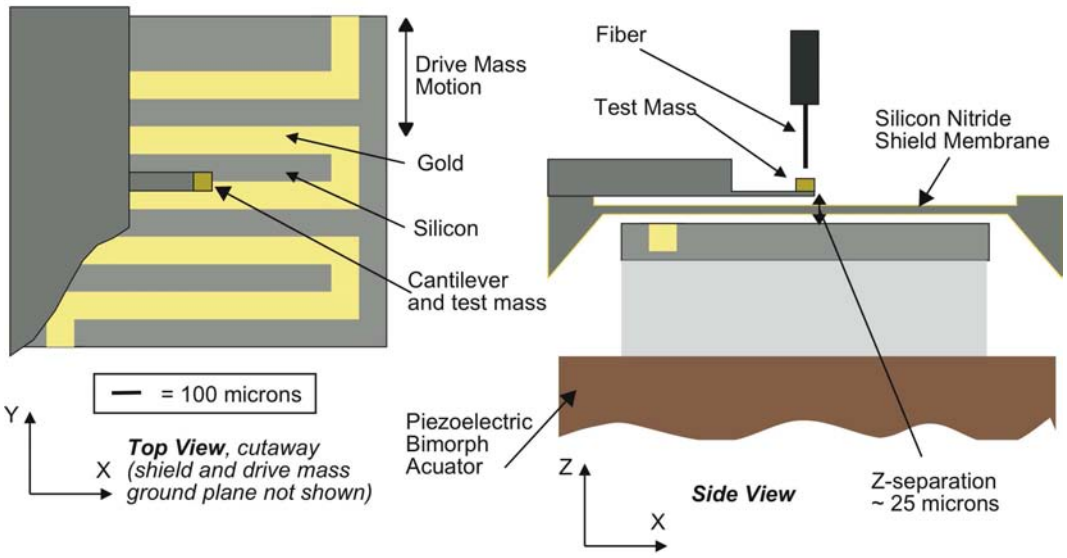

Figure 2: Schematic of the masses and the cantilevers. Geometry in the $x-y$ plane is to scale; the $z-$separation and the thicknesses of the cantilever and shield are not to scale.

In order to make the cantilever move a measureable amount and to isolate the coupling of interest, the cantilever resonance is exploited. Like a spring, the cantilever has a resonant frequency $f_0 = \omega_0/(2\pi)$, determined by its stiffness k, and the mass m of the piece of gold on the end: $\omega_0 = \sqrt{k/m}$. When driven at a finite frequency, the amplitude A of the cantilever's motion at a frequency f is determined by the Lorentzian line shape of the resonance:

$$A(f) = (F/k)\frac{f_0^2}{\sqrt{(f^2 - f_0^2)^2 + \left(\frac{f f_0}{Q}\right)^2}}. \tag{3}$$

Here, F/k is the amplitude of displacement for a dc force F and Q is the quality factor, which is inversely proportional to the damping of the oscillator. When the cantilever is driven on resonance, its motion is enhanced by a factor of Q. To make the cantilever motion large enough to measure, the experiment is designed such that the coupling between the alternating gravitational field and the test mass on the end of the cantilever will drive the cantilever on resonance.

Though driving the cantilever on resonance enhances the amount of motion of the cantilever, the measurement is unavoidably limited by thermal noise. The equipartition theorem and the fluctuation-dissipation theorem yield the force spectral density on the cantilever due to thermal noise at temperature T:

$$F_{min}/\sqrt{b} = \sqrt{(\frac{4kk_BT}{Q\omega_0})}, \tag{4}$$

where the bandwidth b is the inverse of the averaging time and k_B is the Boltzmann constant. Thus, in order to measure a very small force, it is necessary to measure at low temperatures and average for a long time, using a very floppy (low k) and high Q cantilever.

To achieve a high Q, cantilevers are fabricated from single crystal silicon and the experiment is run in vacuum at low temperatures. Only a few microwatts of laser power is used for the interferometric measurement, so as to limit damping of the cantilever due to radiation pressure. Quality factors as high as 80,000 have been achieved at temperatures on the order of 10 K.

The resonant frequency of a cantilever with a test mass is typically near 350 Hz, though this may vary up to 100 Hz between cantilevers. The corresponding spring constant is $k \sim 0.003$–0.009 N/m, orders of magnitude less than

the spring constants of standard commercially-manufactured cantilevers used for atomic force microscopes and other applications. This softness of the cantilevers makes them very sensitive force sensors, though lowering the k too much will cause the cantilevers to droop an unacceptable amount under the weight of the ~ 1.5 μg test mass. With our best cantilevers, averaging for one hour will achieve a thermal noise limit of $F_{min} \sim 10^{-18}$ N, which is a couple of orders of magnitude larger than the ac Newtonian gravitational force at 25 μm separation between the masses.

2.2. Masses

The cantilevers in the experiment are designed to measure very small forces. However, in order to have convincing proof of the functioning of the experiment, a calibration is desirable. To this end, the masses were designed to be functional for a magnetic experiment as well as for the gravitational experiment. Instead of being isolated gold and silicon bars, the drive mass features a gold meander embedded in a silicon substrate. An electrical current passed through the drive mass produces a spatially-varying magnetic field at the test mass. When the drive mass is oscillated underneath the cantilever, there is a time-varying magnetic field at the test mass.

For this magnetic analog experiment, test masses are fabricated with a layer of nickel. The coupling between the magnetic dipole of the test mass and the time-varying magnetic field drives the test mass (and thus the cantilever) in a manner similar to the way a gravitational force is expected to drive the cantilever. Measurement of this magnetic force, orders of magnitude larger than any expected Newtonian or non-Newtonian gravitational force, has provided useful characterization of the apparatus.

Both the test masses and drive masses are made from gold evaporated into cavities that have been plasma-etched in silicon. To make magnetic test masses, a thin layer of nickel is evaporated before the gold. After evaporation, the gold is polished. In the case of the test masses, the silicon is then dissolved, releasing the test masses, which are 50 μm $\times$ 50 μm $\times$ 30 μm in size.

The drive mass, in addition to being a pattern in mass density, presents a spatial periodicity in electrical conductivity. Since this pattern spatially coincides with the periodicity of the gravitational field, a Casimir or electrostatic force between the test mass and the drive mass could mimic a gravitational signal. In order to ensure that there is no such coupling, the drive mass pattern is "buried" under a thin film of gold on the top surface. This gold is grounded and it is electrically isolated from the drive mass pattern by a layer of aluminum oxide. Thus, the drive mass oscillation will create no time-varying electrostatic or Casimir force on the test mass, though the time-varying gravitational field is still present.

2.3. Cantilever and Shield Wafer Assembly

A test mass is glued to a cantilever using a small amount of epoxy. The cantilever wafer die, about 1 cm^2, is then epoxied to a metal wafer-holder, which has a slot into which the optical fiber is guided for the interferometric measurement. A shield wafer is mounted below the cantilever wafer, as shown in Fig. 2. This shield wafer die contains in its center a 3 μm thick membrane of silicon nitride. The entire die, including the shield membrane, is coated with gold on both sides and grounded. The shield membrane, because of its stiffness in comparison to the cantilever and the electrostatic shielding provided by the gold coating, protects the cantilever from being driven by Casimir or electrostatic coupling between the test mass and the drive mass.

2.4. Piezoelectric Bimorph and Vibration Isolation

Though the masses are quite small, the probe itself is much larger, primarily due to the need for vibration isolation. The cantilever is extremely floppy and it is crucial that it is not being mechanically shaken on resonance. The primary source of vibration in the system is the piezoelectric bimorph actuator on which the drive mass is glued. An ac voltage drives the bimorph, oscillating the drive mass underneath the test mass. The bimorph moves on the order of 100 μm; vibration isolation must be such that the base of the cantilever is driven much less than an angstrom on resonance.

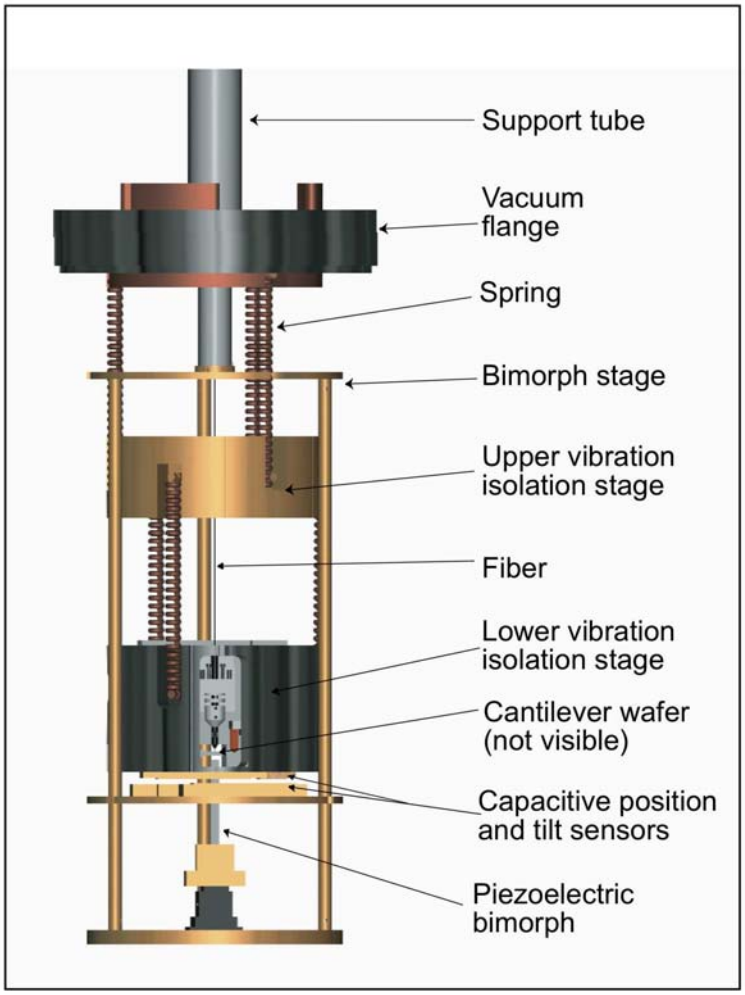

Figure 3: Drawing of the probe, showing the geometry of the cantilever/test mass stage and the bimorph/drive mass stage. The lower vibration isolation stage is stainless steel. The upper stage and the bimorph frame are brass. The entire probe is about 14 inches tall.

To minimize the mechanical coupling between the cantilever and the bimorph on resonance, the bimorph is oscillated at f_{drive}, which is a subharmonic (1/3 or 1/4) of f_0; because of the amplitude of oscillation and the geometry of the drive mass, the time-varying gravitational field will drive the cantilever on resonance (at $3f_{drive}$ or $4f_{drive}$). However, separation of the drive and signal frequencies is not enough. Inherent nonlinearities in the bimorph, as in any piezoelectric, mean that a few percent of its motion will be at higher harmonics. This means that some of the bimorph motion is actually at the resonant frequency of the cantilever. In order to ensure that this nonlinearity is not in fact driving the cantilever mechanically, the bimorph and the cantilever are mounted on two separate stages that are mechanically linked only through two low-frequency spring-mass stages. These simple spring-mass stages provide attenuation on the order of 80 dB at the signal frequency and 60 dB at the drive frequency.

For measurements, the entire cryostat is suspended from the ceiling on springs for additional vibration isolation. This measure is primarily a protection of the experiment from the people in the room; any small jostle of the experiment during data acquisition could smash the drive mass into the shield, destroying the fragile parts of the experiment. Seismic noise is not expected to be of a relevant magnitude at the resonant frequency of the cantilever.

2.5. Alignment

Because the cantilever/test mass assembly and the bimorph/drive mass assembly are mounted on separate stages, care must be taken to align the drive mass underneath the test mass. At room temperature, the cantilever and bimorph stages are adjusted until the drive mass is parallel to the shield and centered in the middle of the shield. Photos of the cantilever and shield wafer during assembly show where the cantilever is located with respect to the middle of the shield. Readings from capacitive position[14] and tilt sensors are recorded at these alignment points. The bimorph stage is then lowered so that the drive mass is far from the fragile shield and cantilever during the cooling and preparation stages of the experiment.

When the system is cooled, the capacitive sensors show that the relative position between the cantilever stage and the bimorph stage changes. The alignment points are regained using a three-axis positioner, which connects via a vacuum feedthrough to the bimorph stage.

Tilt of the cantilever stage with respect to the bimorph stage is adjusted by passing current (typically near 20 mA) through 50 Ω heaters on two of the three BeCu springs from which the cantilever stage is suspended. The bulk modulus of BeCu is strongly dependent on temperature; a small amount of heating is enough to change the length of the springs $\sim 3\%$, adjusting the tilt ~ 3 mrad. This adjustment raises the base temperature of the probe a few degrees, however once the equilbrium temperature is reached, this slightly higher base temperature is not of concern.

Due to limitations of initial optical alignment, there is some uncertainty on the order of 100 μm in the exact $x-y$ alignment between the test mass and the drive mass equilibrium position. The magnetic experiment described above can provide additional information *in situ* about the alignment. However, as described in Sec. 5, magnetic test masses are not used in the more sensitive gravitational experiment.

The vertical separation between the masses is determined by bringing the drive mass slowly into contact with the shield and then backing it off. The contact between drive mass and shield shakes the cantilever, creating a clear signal on the interferometer. As the bimorph stage is lowered, the capacitive position sensor indicates the distance between the drive mass and the shield wafer. The distance between the shield wafer and the cantilever wafer is measured during fabrication. The vertical separation between masses is kept constant during a data run.

2.6. Fiber Interferometer

A fiber interferometer[13, 15] is used to measure the motion of the cantilever. An InGaAs laser diode sends ~ 0.4 mW of 1310 nm light into a fiber coupler. The coupler directs 1% of that light into the fiber pigtail which extends down the length of the dewar. The cleaved end of this fiber is about 50 μm away from the test mass. A few percent of the light reflects from the cleaved end of the fiber and the rest of the light hits the test mass. The space between the cleaved end of the fiber and the shiny surface of the test mass forms a low finesse Fabry-Perot cavity, with a typical visibility of less than 0.5, depending on the quality of the test mass and the alignment between the fiber and the test mass. The reflected light is sent through the fiber coupler to a photodiode wired into a simple transimpedance amplifier with a 10 MΩ feedback resistor.

Because the amplitude of the cantilever motion, on the order of angstroms, is much smaller than the wavelength of the laser light, the interferometer voltage is linearly proportional to the amplitude of cantilever motion. A piezoelectric stack adjusts the equilibrium position of the cantilever to the center of a fringe, where the interferometer is the most sensitive. The noise floor of the interferometer is typically a few $\mu\mathrm{V/Hz}^{1/2}$ or 5–50 $\mathrm{pm/Hz}^{1/2}$.

3. DATA ACQUISITION

Two streams of data are recorded at 10 kHz by a data acquisition card: the voltage signal from the interferometer and the signal from the function generator that is driving the piezoelectric bimorph. Readings from capacitive position and tilt sensors, the thermometer in the probe, and the interferometer reference signal are also continually recorded.

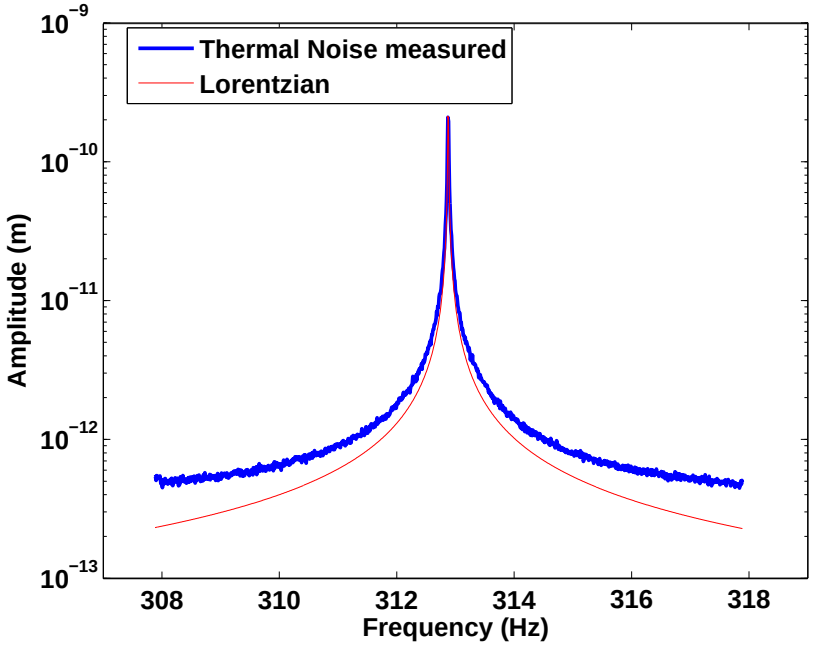

Figure 4: As a function of frequency, the amplitude of cantilever motion due to thermal noise is expected to be a Lorentzian plus a white noise background. In blue are averaged Fourier transforms from 236 consecutive two minute records. In red is the Lorentzian predicted using the measured parameters of the cantilever.

The function generator signal acts as an important timing signal. Any motion of the cantilever that is due to coupling between the test mass and the moving drive mass will be at a definite harmonic of the drive frequency and at a definite phase with respect to the bimorph motion. Analysis of the interferometer data includes a kind of software-based lockin analyis. From each set of time series data, both the interferometer and the function generator signal are Fourier-transformed. The transformed function generator signal will show one peak. From the interferometer data, the Fourier component that corresponds to the proper harmonic of this drive frequency is selected. The amplitude and phase of this Fourier component are considered. Acquiring the raw data as a time series and doing the analysis in software allows multiple harmonics and various noise peaks to be examined in a given data set.

Typical data runs are one hour, with data recorded in many consecutive records of a shorter duration. The length of each record is approximately twice the ringdown time ($\sim 1/Q$) of the cantilever. Each of these shorter records yields a measurement of the Fourier component at the harmonic of the drive frequency. This Fourier component is averaged over the course of the entire data run.

Data are recorded as a function of the equilibrium position (in the y-direction) of the drive mass with respect to the test mass. The force as a function of the alignment between test mass and drive mass is compared to thermal noise and to the expected force between the masses in a Newtonian and Yukawa-type gravitational potential.

Background data are recorded with the drive mass millimeters away from the test mass, with the bimorph on and with the bimorph off. Running the bimorph at a frequency slightly shifted from the subharmonic of f_0 also provides an assessment of background couplings.

4. THERMAL NOISE

The first thing to examine on a cantilever is the thermal noise signal, an indication of the health of the cantilever and the interferometer. Thermal noise data are recorded with the bimorph not moving. A trigger signal may still be recorded from the function generator for purposes of analysis. After averaging, the Fourier transform of the

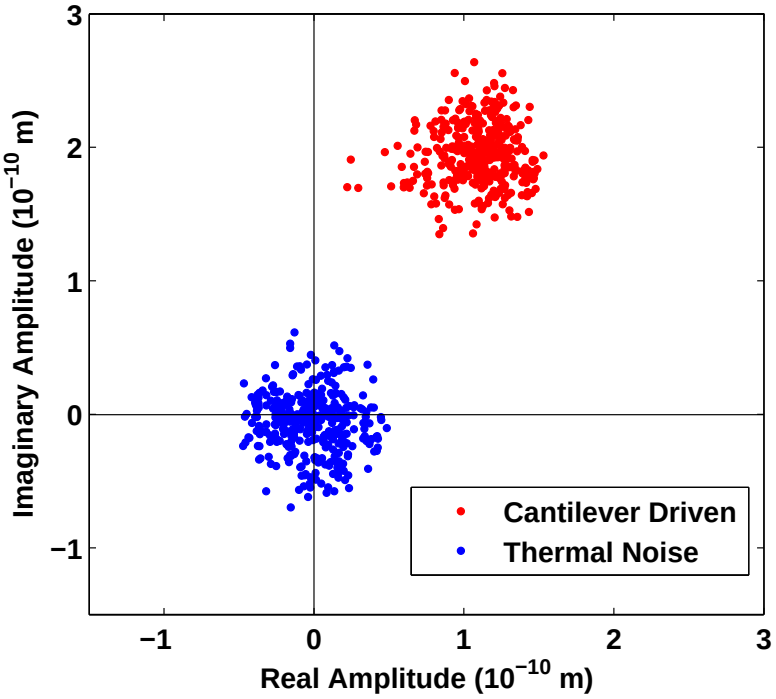

Figure 5: When sampled in the complex plane, thermal noise motion of the cantilever motion at a particular frequency shows a distribution about zero. When the cantilever is driven, the signal gains a definite magnitude and phase, though thermal noise still creates a spread in the measurements about the mean. In data shown, for the purposes of illustration, the cantilever is intentionally driven by a piezo stack with a force much greater than any gravitational force.

interferometer signal does indeed show a thermal noise peak that compares well to the expected Lorentzian, as shown in Fig. 4.

The parameters defining the amplitude and width of the Lorentzian are T, k, and Q of the cantilever. The quality factor is determined by exciting the cantilever and looking at the characteristic ringdown time. The spring constant is determined from the resonant frequency of the cantilever and the mass on the end of it. The temperature is determined by finding the sum square displacement over the thermal noise peak, and using the equipartion theorem: $k < x^2 >= k_B T$. The good fit of the Lorentzian to the observed thermal noise peak is a confirmation of the methods for determining these other parameters.

Thermal noise is random phase noise; it can be thought of as a constant series of "kicks" that the cantilever receives from the thermal bath to which it is attached. The cantilever is continually ringing up and down due to these kicks, though the phase of each kick is random. In the complex plane, a given Fourier component is expected to exhibit a Gaussian distribution centered about zero at any given phase, as shown in Fig. 5. The spread of the distribution is determined by the temperature of the cantilever and the symmetry of the distribution in the complex plane is because of the random phase of each thermal noise "kick." Also because of the random phase, averaging for longer amounts of time reduces the measured force due to thermal noise; as described in Eqn. 4, the thermal noise force scales as $1/\sqrt{t}$, where $t = 1/b$ is the averaging time. As evident in Fig. 5, thermal noise adds a statistical uncertainty to the measurement of a coherent force; thus, longer averaging times are important for precise force measurements.

5. SOURCES OF BACKGROUND

Because the gravitational force is very small, great care must be taken in the experimental design to minimize background forces. Many source of background, such as the earth's gravitational field or the Casimir force between the shield and test mass, are dc and thus do not affect the finite-frequency measurement in the experiment. As described above, external and internal springs provide vibration isolation. The grounded plane on top of the drive mass and the shield between test and drive masses isolate the test mass from any finite frequency electrostatic or Casimir couplings. Though the magnetic analog to the gravitational experiment has been very useful and informative, it is necessary to use non-magnetic test masses for a more sensitive gravitational measurement. Due to the difference in the magnetic susceptibility between gold and silicon, a magnetic test mass will act as a susceptometer, thus indicating the presence of a force much larger than gravity. Using a non-magnetic test mass easily eliminates this source of background.

The largest remaining source of background is the interferometer itself. Johnson noise on the large feedback resistor of the interferometer circuit and white noise on the laser current source provide a negligible white noise background. Finite reflections from all the connectors in the interferometer circuit become stray interferometric signals that add sub-Hz noise to the signal; these effects may be reduced by modulation of the laser at $\sim$ 100 MHz, which reduces the coherence length of the laser and thus the importance of the very long paths between the optical connectors. Because the much smaller cavity between the cleaved fiber end and the test mass remains shorter than the coherence length of the laser, this modulation does not significantly reduce the signal of interest.

Of most concern is any noise that is at the cantilever resonant frequency, in particular any noise that is at a constant phase with respect to the driving signal. Direct electrical pickup of harmonics of the drive frequency would be one such example. A second method for such pickup is mechanical coupling: if the optical fiber is vibrated by the motion of the bimorph, this will create optical noise due to the changing lengths of any stray interferometric paths. Non-linearities in the bimorph or mechanical non-linearities in the optical fiber mean that the fiber may indeed shake at harmonics of the driving signal, thus creating a coherent signal at the cantilever resonance. Such coupling on the interferometer, like the low frequency noise, is reduced by modulation of the laser.

6. DISTINGUISHING A GRAVITATIONAL SIGNAL

In contrast to thermal noise, a coherent driving force on the cantilever will show a definite phase and magnitude when a particular Fourier component is plotted in the complex plane. Over the course of one data run, each shorter time-series record yields one point in the complex plane. The distribution of these points in the complex plane and the behavior of a force as a function of averaging time indicate whether thermal noise or a coherent force is present. A coherent force could be non-Newtonian gravitational coupling between the drive mass or it could be an unanticipated background force. A key to distinguishing a true mass coupling from a background force is to vary the equilibrium position (along the y-axis) of the oscillating drive mass with respect to the test mass. As shown in Fig. 6, there is a clear periodicity in the dc gravitational force across the drive mass pattern and this creates a periodicity in the measured ac force.

The primary part of the drive mass pattern is 1 mm long, including five 100 μm wide gold bars. *In situ*, the drive mass is oscillated at an amplitude of only $\sim$ 120 μm. The drive mass may be positioned so that at the equilibrium position of its oscillation, a gold bar is centered underneath the test mass. Or it may be positioned such that the boundary between a gold bar and a silicon bar is underneath the test mass. Such a change in equilibrium position of 50 μm makes a distinct change in the force on the test mass at a given harmonic of the drive frequency. Indeed, finite element analysis shows that the third harmonic force is at a minimum when the test mass is centered over a gold bar or a silicon bar at the equilibrium and it is a maximum when the test mass is centered over the gold/silicon boundary. Moreover, the phase of the signal with respect to the drive is expected to show a discontinuous phase change of π at every force minimum. This periodicity of the force, in magnitude and phase, is illustrated in Fig. 7.

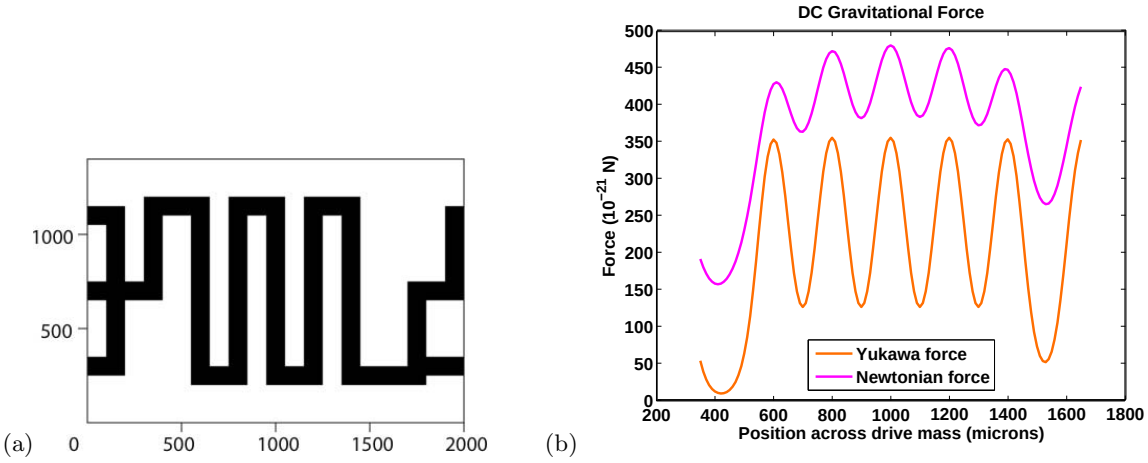

Figure 6: (a) The drive mass pattern, with black representing the gold part. Scales are shown in microns. (b) The dc gravitational force as a function of position along the long axis (referred to as the y-direction, shown as horizontal in this diagram) of the drive mass, when centered along the short axis. Note that the Yukawa force (shown here for $\alpha = 5$ and $\lambda = 18$ μm) is smaller in magnitude but steeper than the gravitational force.

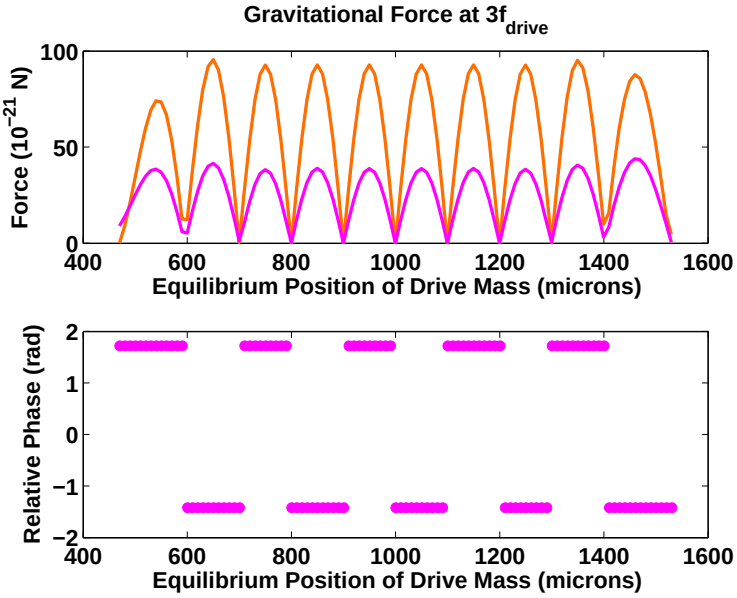

Figure 7: From finite element analysis, the force (top) and phase (bottom) of the predicted ac gravitational signal at the third harmonic of the drive frequency. Note that the magnitude and steepness of the curves depend on α and λ, amplitude of drive mass oscillation, and separation between drive mass and test mass. However, the same periodicity of 100 μm in the force and the discontinuities of π in the phase are always present. The Yukawa force for $\alpha = 5$ and $\lambda = 18$ μm is shown in orange; the Newtonian force is in pink. The phase is the same for a Newtonian or a Yukawa force.

Any force that is a true coupling between the drive mass and the test mass will have a periodicity as a function of the drive mass equilbrium position along the y-direction. Though thermal noise, always finite, adds a statistical uncertainty that prevents an accurate measurement of the force minima, any coupling between the masses that is well above thermal noise at its maxima should show an obvious periodicity. For example, the force in the magnetic analog experiment described above is expected to show a distinct pattern, though it has a spatial periodicity of 200 μm instead of 100 μm; this was easily and clearly demonstrated in experiments with the magnetic test mass.

If a force measured as a function of equilibrium position does not show the expected periodicity, then the possibility

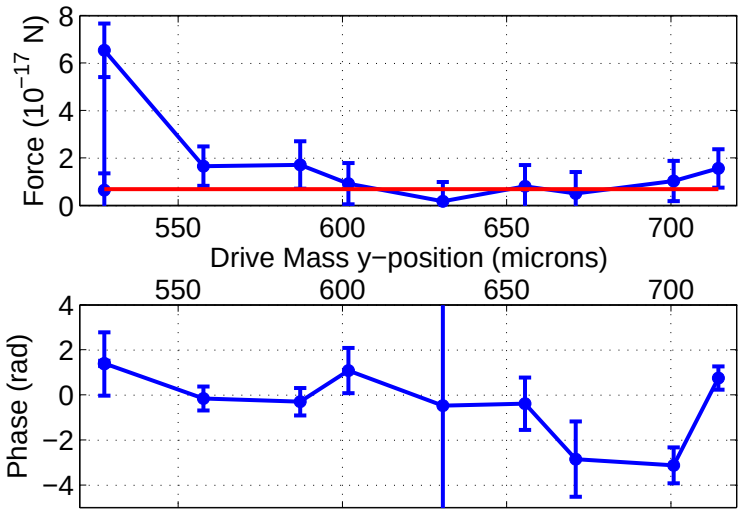

Figure 8: The force (top) and phase (bottom) of the measured ac gravitational signal as a function of drive mass equilibrium position during one experimental run. The red line shows the thermal noise level and the error bars show two standard deviations of statistical uncertainty. Error bars that go below zero on the force and outside of the shown range of phase are truncated. Analysis of data is preliminary and data are shown primarily for the purposes of illustration. Note the anomalously high force measured at the first point was not present upon a second measurement.

of deviations from Newtonian gravity at the level of the measured force can easily be dismissed. For example, the earlier published data from this experiment [7] showed no significant change in the force as the equilbrium position was changed and thus it was concluded that the measured force was a spurious background. More recent data, such as those shown in Fig. 8, show that improvements to the apparatus have reduced many sources of background. Moreover, the recent results include more measurements of force as a function of equilbrium postion, allowing for more sophisticated analysis and a better determination of the limits on α and λ from this experiment.

In the experimental run summarized in Fig. 8, the measured force was found to hover around thermal noise. Neither the magnitude nor the phase was found to show any clear periodicity. One way to set a bound on Yukawa-type deviations from Newtonian gravity is to simply consider the maximum measured force. This measured force (plus the accompanying statistical uncertainty) may be set equal to the local maximum of a force arising from a Newtonian potential plus a Yukawa potential; a bound on α and λ is derived from this equality. However, such an analysis does not use all the information available. Another way to use these data is to find a best fit between the measured force as a function of equilibrium position and the kind of predictions shown in Fig. 7. Such a comparison uses the entire data set to determine with what α and λ a Yukawa potential could create a force of the measured magnitude and phase. This consideration of the geometry of the system allows for a sort of spatial lockin analysis, a powerful tool in analyzing any measured force and setting a bound on $\alpha(\lambda)$. A bound derived from such a fit is expected to be more appropriate than, though quantitatively similar to, a bound derived from only the maximum measured force.

7. FUTURE IMPROVEMENTS

The data shown in Fig. 8 show a force close enough to thermal noise that it is difficult to determine if there is any periodicity. The latest results, not shown, include a lower thermal noise limit, better alignment between the optical fiber and the test mass, and less uncertainty in the alignment between the drive mass and the test mass. These

results represent roughly an order of magnitude improvement in comparison to currently published results. Even better results could be gained with longer averaging times, a further reduction in the mechanical coupling between the bimorph and the interferometer, a closer approach between drive mass and test mass, and the reintegration of a magnetic calibration.

The power of the spatial lockin analysis is reduced by uncertainty in the relative $x - y$ distance between the test mass and the drive mass equilibrium position. The magnetic analog experiment could reduce this uncertainty. With this in mind, a cantilever with a patterned metallized loop is being developed in order to provide a magnetic dipole that may be turned on (by passing a current through the loop) for a magnetic calibration and turned off for a sensitive gravitational measurement. No magnetic test mass is needed for such an experiment. Fabrication of these cantilevers is in progress.

To investigate the possibility of $\alpha(\lambda)$ at a couple of orders of magnitude lower than what the current apparatus will measure, a second generation of this experiment is being designed. This new version utilizes a rotational instead of a linear drive, which affords many geometrical advantages in the measurement. Additionally, because the cantilever wafer is fixed into position with respect to the spinning drive mass, the new design avoids many of the practical challenges of alignment that are limitations of the present design.

8. CONCLUSION

The apparatus described in this paper is able to measure the force between masses separated by as little as 25 μm. Sensitivity is enhanced by using a floppy, high Q cantilever at low temperatures. Separation of the signal frequency from the drive frequency and measurement of the force as a function of the equilibrium position of the drive mass with respect to the test mass allows for clear discrimination of coupling between the masses from spurious background forces. This measurement is a new test of physics beyond the Standard Model at the 25 μm length scale, providing a constraint on deviations from Newtonian gravity as predicted by theories of exotic particles and extra dimensions.

Acknowledgments

This work is supported by National Science Foundation contract NSF-PHY-0244932.

References

[1] S. Dimopolous and G. F. Guidice, "Macroscopic forces from supersymmetry," Phys. Lett. B **379**, 105 (1996).
[2] R. Sundrum, "Towards an effective particle-string resolution of the cosmological constant problem," J. High Energy Phys. **07**, 001 (1999).
[3] D. B. Kaplan and M. B. Wise, "Couplings of a light dilaton and violations of the equivalence principle," J. High Energy Phys. **08**, 037 (2000).
[4] N. Arkani-Hamed, S. Dimopoulos, and G. Dvali, "Phenomenology, astrophysics, and cosmology of theories with submillimeter dimensions and TeV scale quantum gravity," Phys. Rev. D **59**, 086004 (1999).
[5] C. D. Hoyle, D. J. Kapner, B. R. Heckel, E. G. Adelberger, J. H. Gundlach, U. Schmidt, and H. E. Swanson, "Submillimeter tests of the gravitational inverse-square law," Phys. Rev. D **70**, 042004 (2004).
[6] J. C. Long. H. W. Chan, A. B. Churnside, E. A. Gulbis, M. C. M. Varney, and J. C. Price, "Upper limits to submillimetre-range forces from extra space-time dimensions," Nature **421**, 922 (2003).
[7] J. Chiaverini, S. J. Smullin, A. A. Geraci, D. M. Weld, A. Kapitulnik, "New experimental constraints on non-Newtonian forces below 100 μm," Phys. Rev. Lett. **90**, 151301 (2003).
[8] S. K. Lamoreaux, "Demonstration of the Casimir force in the 0.6 to 6 μm range," Phys. Rev. Lett. **78**, 5 (1997).

[9] S. Hannestad and G. G. Raffelt, "Stringent neutron-star limits on large extra dimensions," Phys. Rev. Lett. **88**, 071301 (2002).

[10] E. G. Adelberger, B. R. Heckel, A. E. Nelson, "Tests of the gravitational inverse-square law," Ann. Rev. Nucl. Part. Sci. **53**, 77 (2003).

[11] S. Beane, "On the importance of testing gravity at distances less than 1 cm," Gen. Rel. Grav. **29**, 945 (1997).

[12] S. Dimopoulos and A. A. Geraci, "Probing submicron forces by interferometry of Bose-Einstein condensed atoms," Phys. Rev. D **68**, 124021 (2003).

[13] J. Chiaverini, "Small force detection using microcantilevers: Search for millimeter range deviation from Newtonian gravity," PhD thesis, Stanford University, 2002.

[14] S. B. Field and J. Barentine, "Capacitive position sensor with simultaneous linear X-Y readout," Rev. Sci. Instrum. **71**, 2603 (2000).

[15] D. Rugar, H. J. Mamin, and P. Guethner, "Improved fiber-optic interferometer for atomic force microscopy," Appl. Phys. Lett. **55**, 2588 (1989).